

## 15. SPECIAL ASTROMETRY AND PHOTOMETRY OF SOLAR SYSTEM OBJECTS

*Solar system objects were observed by the star mapper if they were sufficiently bright and sufficiently small in angular size. This resulted in a list of positional observations by Tycho of 5 minor planets, 3 satellites and 2 major planets, and their estimated  $B_T$  and  $V_T$  magnitudes. The adaptation of the reduction algorithms for the planetary objects is outlined in this chapter, and the reduction of pairs of successive observations on the inclined and vertical slits to obtain two-dimensional positions on the sky is presented. The precision and accuracy of the Tycho results are discussed in a comparison with Hipparcos and ground-based observations.*

---

### 15.1. General Overview of Planetary Data Treatment

---

The proper acquisition and reduction of Tycho observations of planets was recognized as an important task for the Tycho Consortium. Although the precision of these observations is moderate compared to the Hipparcos main mission data (see Volume 3, Chapter 15), Tycho astrometry and photometry have some advantages which made it a worthwhile task. Each passage of a planet across the inclined, and then the vertical slits of the star mapper provides a nearly simultaneous determination of the position of the object in two dimensions in the tangential plane, while the main grid position determination is always one-dimensional, see Section 2.7.2 of Volume 1. Regarding astrometry of planets, observations on the inclined slits become particularly interesting since measurements only along the scanning direction, as obtained by the main grid and the vertical slits of the star mapper, cannot provide the ecliptic longitudes of objects in the ecliptic zone nearly as accurately as the latitudes, due to the features of the scanning law. The width of the star mapper slits in the scan direction is significantly larger than that of the main grid, allowing four planets and satellites of larger angular size to be observed (Uranus, Neptune, Ganymede and Callisto). Last but not least, the two-dimensional position determinations are supplemented by simultaneous photometric observations in the  $B_T$  and  $V_T$  passbands for all but the largest planets.

Since rapidly moving planets could not be treated with the same model of five astrometric parameters as ordinary programme stars, several major changes had to be made in some of the principal stages of the data processing. The prediction of transit times was designed and implemented specially for planetary objects, as described in Section 10.4. The resulting Predicted Group Crossings were merged in chronological sequence with

the predictions for programme stars, constituting the input for the detection and transit identification procedures, including parasite recording. These latter did not distinguish between planets and stars and remained unchanged. In the identified transit data stream the transits of planets could be recognized easily by special object designations resembling Tycho Input Catalogue identification numbers (see Chapter 3), but having zeroes in the place of the Guide Star Catalog region numbers. The format and the structure of the data were exactly the same otherwise.

In the astrometric reduction, the existing routine procedures of the Tycho data processing were retained whenever possible. For that reason a dummy entry was created for each planetary object in the Star Constants Catalogue for reprocessing. The five astrometric parameter updates (Section 11.1) were kept null throughout the processing. In this way, the transits of planets could be drawn through the same stages of the main astrometric reductions, including filtering of low-quality observations, correction of residuals transit times for calibration parameters, astrometric updates (always zero in this case), etc.

At the point where the observation equation was calculated, a few input data parameters and computed terms were written in a special 'planet observations' file. One record of this file corresponded to one detected transit of a planet. Each record contained the following data:

- the object's identification number;
- the predicted transit time in the Terrestrial Time (TT) scale;
- the first two coefficients of the observational equation (Equation 15.1);
- the corrected astrometric residual in arcsec;
- the astrometric weight of the observation, corresponding to  $\sigma_u$  in arcsec;
- the signal amplitude in the  $B_T$  and  $V_T$  passbands;
- slit group flags;
- All-Transits (AT) flags (see Sections 7.4, 11.4 and 12.3), related to the astrometric quality of the observation;
- the position angle of the scan direction,  $\theta$ .

The planet observations file was not self-contained since only a correction to the ephemerides position could be directly derived from its contents, but not the observed position itself. The complete planet observations file was therefore returned to the prediction processing site in Heidelberg, to be supplemented with the predicted apparent positions. The actual time of observation instead of the predicted transit time was also computed, taking into account once again the actual spin velocity of the satellite. This modified planet observations file was a self-contained set of information for the final determination of equatorial coordinates, standard errors and other relevant data, as described in more detail in the next section. The final coordinates are independent of the ephemerides used in prediction.

The observed  $B_T$  and  $V_T$  magnitudes were calculated directly from the amplitudes in the planet observations file by a simplified calibration procedure. The user should be aware of systematic errors of these magnitudes for objects with angular diameters which are not small compared to the slit width. For such objects a dedicated study is required, taking into account the single-slit response functions (Section 1.5), the Tycho estimation process (Section 4.4) and the phase and limb darkening of the object.

---

## 15.2. Reduction of Planet Observations

---

The primary astrometric information about the position of a given object is contained in the transit time. The transit time  $\tau$  is the moment, derived in the detection and estimation process (Chapter 4), when the object crosses the fiducial line of the slit group. By definition, the projected along-scan distance  $u(t)$  of the object from the slit group is zero at the transit time,  $u(\tau) = 0$ . In all Tycho data reductions, the observed transit time  $\tau$  was compared with the predicted time of group crossing  $\tau_{\text{calc}}$ , calculated from a suitable ephemeris, the current grid calibration parameters and satellite attitude at the calculated time of transit  $\tau_{\text{calc}}$ . It follows that the observed difference in along-scan distance is  $\Delta u = u_{\text{obs}} - u_{\text{calc}} = -v_{\text{scan}}(\tau_{\text{obs}} - \tau_{\text{calc}})$ , (Equation 7.5).

The observation equation for a star crossing one slit group is given by Equation 7.4. When adjusted to a planet, crossing one slit group, the equation is simpler since only  $(\Delta\alpha, \Delta\delta)$  are unknowns. It is noted that the instrumental calibration terms, great-circle zero point corrections and correction for the movement in the  $z$  direction have been subtracted in the right-hand part of the equation, in the same way as for ordinary stars.

We define the calculated position of the planet at the inclined slit at the calculated time of transit  $t_1$  ( $t_1; \alpha_1, \delta_1$ ) and similarly ( $t_2; \alpha_2, \delta_2$ ) for the following vertical slit group. The resulting two observation equations in general form are:

$$\frac{\partial u}{\partial \alpha^*} \Delta \alpha^* + \frac{\partial u}{\partial \delta} \Delta \delta + \text{noise} = \Delta u \quad [15.1]$$

where  $\Delta \alpha^* = \Delta \alpha \cos \delta$ . Assuming that the ephemeris used by prediction is sufficiently accurate for the calculation of the planet motion during the short interval  $t_2 - t_1$ , one can rewrite the observational equations in the following form:

$$\begin{aligned} A_1 \Delta \alpha_{2^*} + B_1 \Delta \delta_2 &= \Delta u_1 \\ A_2 \Delta \alpha_{2^*} + B_2 \Delta \delta_2 &= \Delta u_2 \end{aligned} \quad [15.2]$$

for a pair of sequential observations on the inclined and vertical slits (called an elementary observation hereafter), where  $\Delta \alpha_{2^*}$  and  $\Delta \delta_2$  are unknown corrections to the equatorial coordinates of the planet at the calculated epoch  $t_2$ , which are chosen arbitrarily as the reference epoch of the elementary observation. The right-hand parts are the observed and corrected along-scan distances. The coefficients can be written for the inclined slit as:

$$\begin{aligned} A_1 &= \frac{\partial u_1}{\partial \alpha^*} = \sin \theta - \text{sign}(z) \cos \theta \\ B_1 &= \frac{\partial u_1}{\partial \delta} = \cos \theta + \text{sign}(z) \sin \theta \end{aligned} \quad [15.3]$$

and for the vertical slit as:

$$\begin{aligned} A_2 &= \sin \theta \\ B_2 &= \cos \theta \end{aligned} \quad [15.4]$$

where  $\theta$  is the position angle of the  $w$  axis (see Figure 15.1),  $\text{sign}(z)$  is the sign of the  $z$  coordinate ( $-1$  for the lower branch of inclined slits and  $+1$  for the upper).

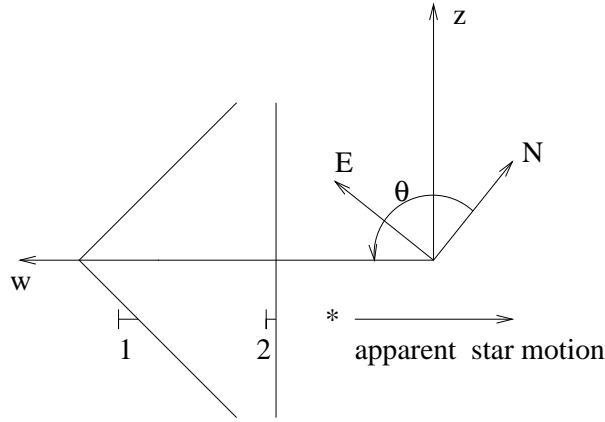


**Figure 15.1.** The star mapper coordinate system ( $w, z$ ). The position angle  $\theta$  from prediction is illustrated for a given direction of north. The observations  $\Delta u_1$  and  $\Delta u_2$  are indicated at 1 and 2.

Then, directly from Equations 15.2:

$$\begin{aligned}\Delta\alpha_{2*} &= \text{sign}(z)(B_1\Delta u_2 - B_2\Delta u_1) \\ \Delta\delta_2 &= -\text{sign}(z)(A_1\Delta u_2 - A_2\Delta u_1)\end{aligned}\quad [15.5]$$

The variances in equatorial coordinates can be obtained from the above formulae:

$$\sigma_{\alpha_*}^2 = B_1^2\sigma_2^2 + B_2^2\sigma_1^2 \quad [15.6a]$$

$$\sigma_\delta^2 = A_1^2\sigma_2^2 + A_2^2\sigma_1^2 \quad [15.6b]$$

where the standard deviations  $\sigma_1$  and  $\sigma_2$  are given in the planet observations file.

Finally, it should be noted that the derived corrections to the coordinate components in general are not statistically independent. The covariance is:

$$\begin{aligned}C(\alpha_*, \delta) &= -A_2B_2\sigma_1^2 - A_1B_1\sigma_2^2 \\ &= -\sigma_1^2 \cos\theta \sin\theta + \sigma_2^2 \text{sign}(z)(\cos^2\theta - \sin^2\theta)\end{aligned}\quad [15.7]$$

The correlation coefficient is calculated as:

$$\rho_{\alpha_*\delta} = \frac{C(\alpha_*, \delta)}{\sigma_{\alpha_*}\sigma_\delta} \quad [15.8]$$

Each published elementary astrometric observation is completely described by the derived position  $(\alpha_{\text{obs}}, \delta_{\text{obs}})$ , the epoch  $t_2$ , standard errors  $\sigma_{\alpha_*}$  and  $\sigma_\delta$  and correlation  $\rho_{\alpha_*\delta}$ . In addition, the position angle  $\theta$ , slit flag  $\text{sign}(z)$  and standard errors  $\sigma_1$  and  $\sigma_2$  are given to enable future systematic corrections of the data.

---

### 15.3. Accuracy and Precision

---

A full comparison of Tycho astrometric data for solar system objects with on-ground observations of the same epoch is given below. It is noted that the results are quite compatible in that the Tycho accuracy is close to or slightly better than that achieved in the best on-ground observations at the Bordeaux and Carlsberg meridian circles. The Tycho observations are complementary since they cover periods around the quadratures while meridian circle observations are obtained around opposition.

At the same time, as can be seen from Figures 15.2–15.9, the real uncertainty of Tycho observations, reflected in the scatter, is significantly larger than the formal standard errors (error bars). A few features of the astrometric reduction as well as the intrinsic characteristics of the objects explain this discrepancy.

The images of planets are broader and more flat at the tops than the diffraction limited images of stars. But the formal errors were still derived by means of the same error model (Makarov & Høg 1995) which is adequate for stellar images only. This especially concerns Uranus, Neptune and the two Jovian satellites. In fact, the error model is not applicable to extended objects at all. The differences in the error bars are due to variations of the detected amplitude or sky background but the broadening of the image gives the larger effect. Accidental proximity of parasitic stars also disturbs observations, as mentioned in Section 2.7 of Volume 1, but for the 10 rather bright objects the effect is relatively moderate. We conclude that the standard errors  $\sigma_1$ ,  $\sigma_2$ ,  $\sigma_{\alpha^*}$  and  $\sigma_\delta$  given among the published data can serve only as approximate indicators of the observation quality. In particular, the error ellipse described in Section 2.7 cannot be regarded as an estimation of a certain confidence range in the sense usually attributed to it (see e.g. Press *et al.* 1986, Section 14.5).

As far as systematic errors are concerned, it is noted that the positions are strictly tied to the ICRS system, and large-scale distortions of the Tycho coordinate system are estimated to be as small as 1 mas. Yet, there are much larger intrinsic systematic errors in the data due to physical and geometrical phase effects, i.e. phase, shape or albedo corrections are not taken into account. It is possible to apply this correction afterwards in the case of Tycho, and here follows a general description of how it might be achieved. A discussion of these effects is given by Lindegren (1977) for observations with a slit micrometer on a meridian circle, very similar to the Tycho instrument. The method was applied to observations by Lindegren & Høg (1977). As applied to the Tycho observations the method translates into a series of numerical simulations.

For any given observation of a planet, two two-dimensional images can be simulated, one image as a star-like source, and another as a disk with realistic phase, shape and albedo. These two images should be transformed into simulated Tycho counts by integration in the along-slit direction, convolution with the slit response function (Figure 1.3) and discretisation of the resulting 4 profiles into 0.281 arcsec bins, which is a sufficiently accurate approximation for the purpose. To do these computations, the position angle  $\theta$  and the inclined slit flag  $\text{sign}(z)$  should be used. The next step would be to apply the detection Q-filter to the 4 digitized profiles, that is explicitly  $[1, 1, 1, 0, -1, -1, -1]$  (see Section 4.3). Following the steps of the detection processing, the transit time is derived from the filtered counts by simple linear interpolation between two adjacent counts where the value changes from negative to positive. Then the whole procedure of coordinate determination should be repeated, as described in the previous section, taking the differences in transit times instead of the residuals  $\Delta u_1$  and  $\Delta u_2$  for inclined and vertical slit crossings, respectively. The resulting  $\Delta\alpha^*$  and  $\Delta\delta$  are the required systematic corrections to the observed equatorial coordinates. In principle the same simulations could be used to correct the  $B_T$  and  $V_T$  magnitudes.

To assess the validity of astrometry for the solar system objects, the Tycho positions were compared to other observations and to calculated positions from the ephemerides. A first comparison was made between the Hipparcos and the Tycho positions for the 6 solar system objects which are in common with the two catalogues (five minor planets and the planetary satellite S VI-Titan). As the transits across the star mapper and the main grid

occurred almost simultaneously, a direct comparison between the Tycho and Hipparcos observations could be achieved. The Tycho positions were transformed into a one-dimensional abscissa and were corrected for the epoch offset between the observations ( $\simeq 11$  s), assuming a constant velocity  $dv/dt$  calculated from the ephemeris. The residual  $\Delta v$ , i.e. the difference between the Tycho and Hipparcos abscissa on a great circle, is given by (see Section 2.7 of Volume 1):

$$\Delta v = v^{\text{Tycho}} - v^{\text{Hip}} \simeq (\sin \theta \quad \cos \theta) \begin{pmatrix} (\alpha - \alpha_0) \cos \delta \\ \delta - \delta_0 \end{pmatrix} + (t_{\text{Hip}} - t_{\text{Tycho}}) dv/dt \quad [15.9]$$

where  $\theta$  is the position angle of the FAST or NDAC reference great circle,  $(\alpha, \delta)$  are the equatorial coordinates from Tycho at epoch  $t_{\text{Tycho}}$ , and  $(\alpha_0, \delta_0)$  is the reference position of the Hipparcos solar system objects catalogue at epoch  $t_{\text{Hip}}$ . The normalized difference is derived from the approximation:

$$\sigma_{\Delta v} \simeq [(\sin \theta \sigma_{\alpha^*})^2 + (\cos \theta \sigma_{\delta})^2 + \sin 2\theta \rho_{\alpha^* \delta} \sigma_{\alpha^*} \sigma_{\delta}]^{1/2} \quad [15.10]$$

since the variance of the Hipparcos measurements can be neglected here.

The one-dimensional differences are shown for all objects in common as a function of epoch on top of Figure 15.2(a); the lower panel shows an histogram of the normalized difference with the theoretical Gaussian of same mean and variance as the data sample. Similar graphs are obtained for each object at the top of Figures 15.3 to 15.8. Figure 15.2(b) and Figures 15.3 to 15.9 show the residuals  $\Delta \alpha \cos \delta$  and  $\Delta \delta$  between the observed and calculated astrometric positions obtained for each Tycho solar system object. These are given together with the residuals provided by L.V. Morrison for the Carlsberg instrument observations, and residuals obtained by M. Rapaport at the Bordeaux Observatory. The ephemerides of the minor planets were computed according to the osculating elements set of the 'Ephemerides of minor planets for the year 1996' (Batrakov *et al.* 1995). The ephemerides of the major planets are given by DE200 except for S VI-Titan where they are calculated from the DE403 solution. The ephemerides of the Galilean satellites are taken from the G5 theory of Arlot (1982), the ephemerides for S VI-Titan are taken from the theory of Dourneau (1993) for Tycho and the more recent theory TASS1.6 of Vienne & Duriez (1995) for the Bordeaux observations.

The scatter on the residuals for the major planets is greater than expected from the formal error on a single observation; it is however stressed that all positions for any solar system object refer to the combination of the slits group crossing positions without any correction for photocentre offset due to phase effect. The systematic offset on the residuals in right ascension for the major planet is in agreement with the ground-based observations and known to be mainly due to the DE200 ephemeris.

E. Høg, D. Hestroffer, V.V. Makarov

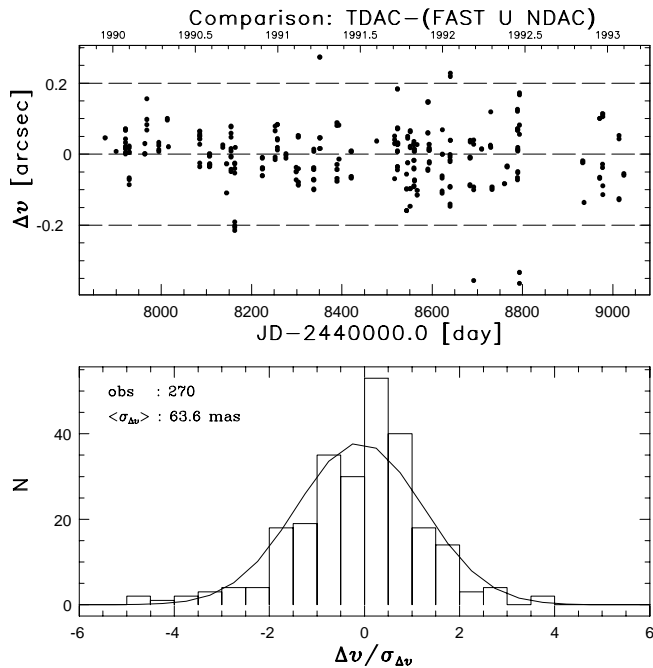


**Figure 15.2(a).** Comparison between Tycho and Hipparcos abscissae for five minor planets and S VI-Titan. The one-dimensional differences are given as a function of epoch in the top panel. The lower panel gives the distribution in units of the scatter, the number of observations and the mean standard deviation  $\langle \sigma_{\Delta V} \rangle$ .

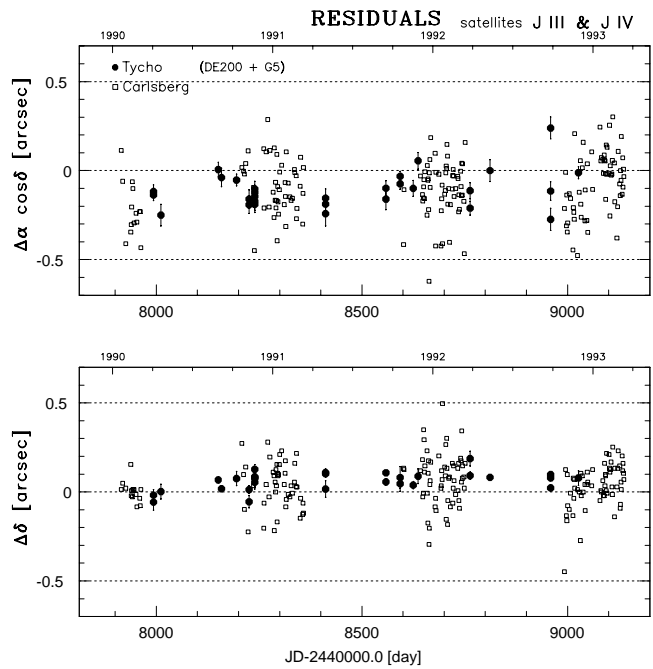


**Figure 15.2(b).** Residuals for Tycho observations of the Galilean satellites J III-Ganymede and J IV-Callisto, together with residuals obtained from Carlsberg instrument observations.

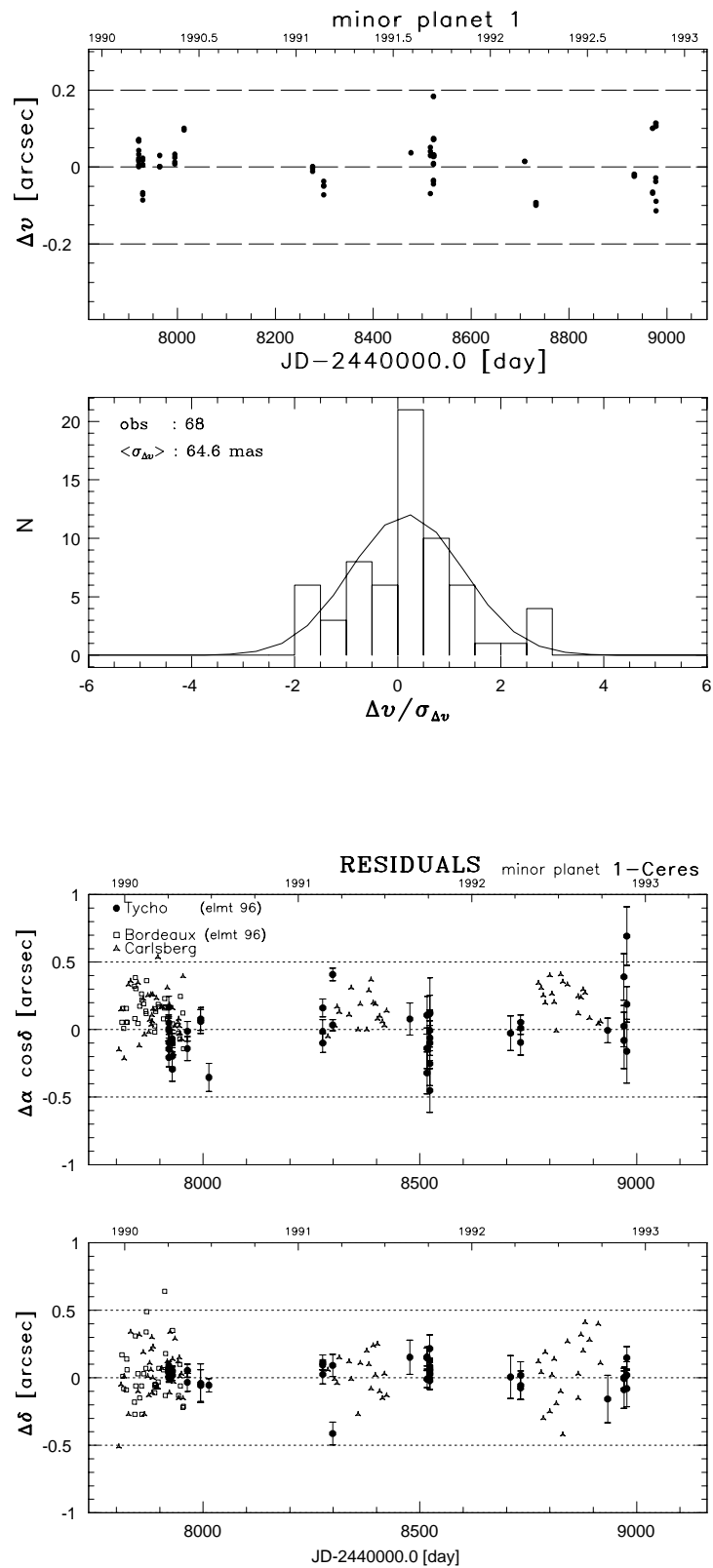


**Figure 15.3.** Residuals for Tycho observations of (1) Ceres together with residuals obtained from ground-based observations (lower), and residuals with respect to Hipparcos results (upper). The Bordeaux and Carlsberg data and residuals were provided by M. Rapaport and L. V. Morrison.



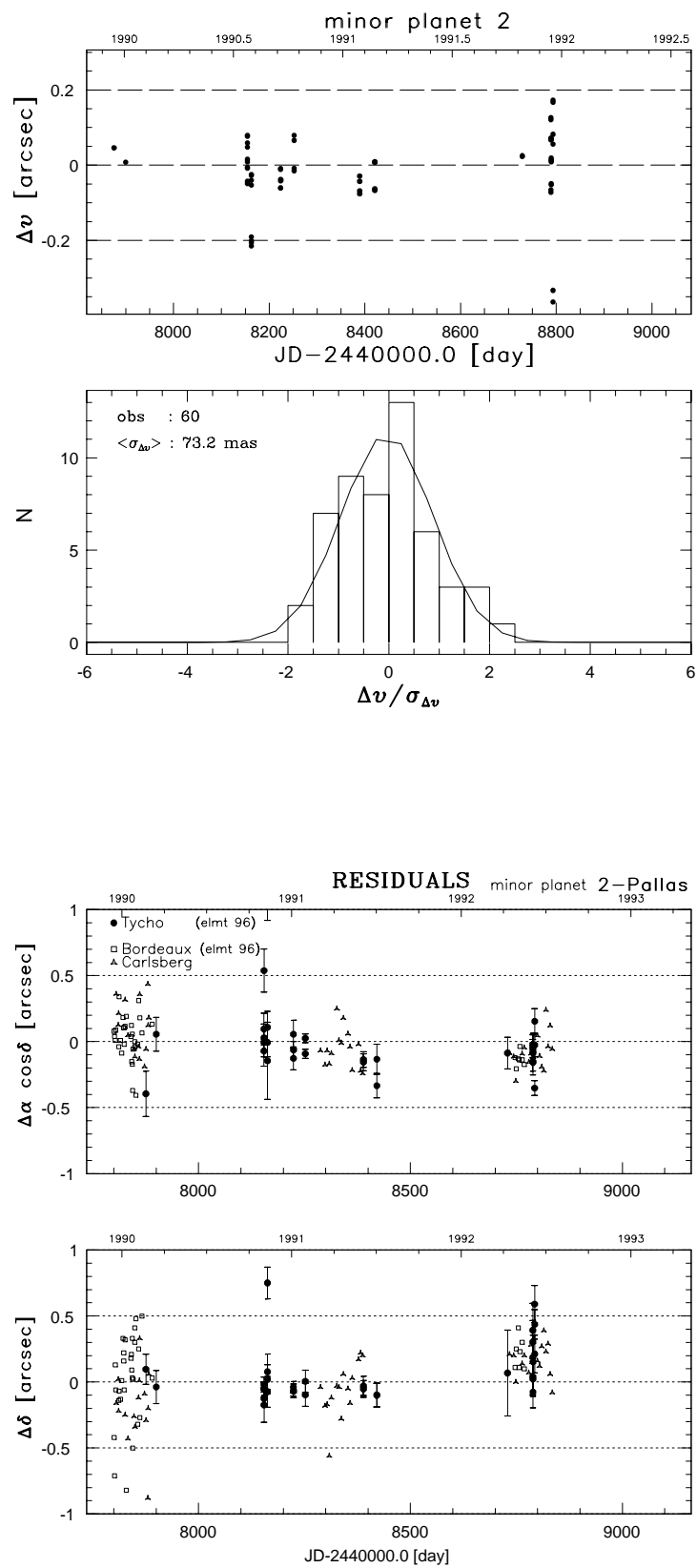


Figure 15.4. Same as Figure 15.3 for (2) Pallas.

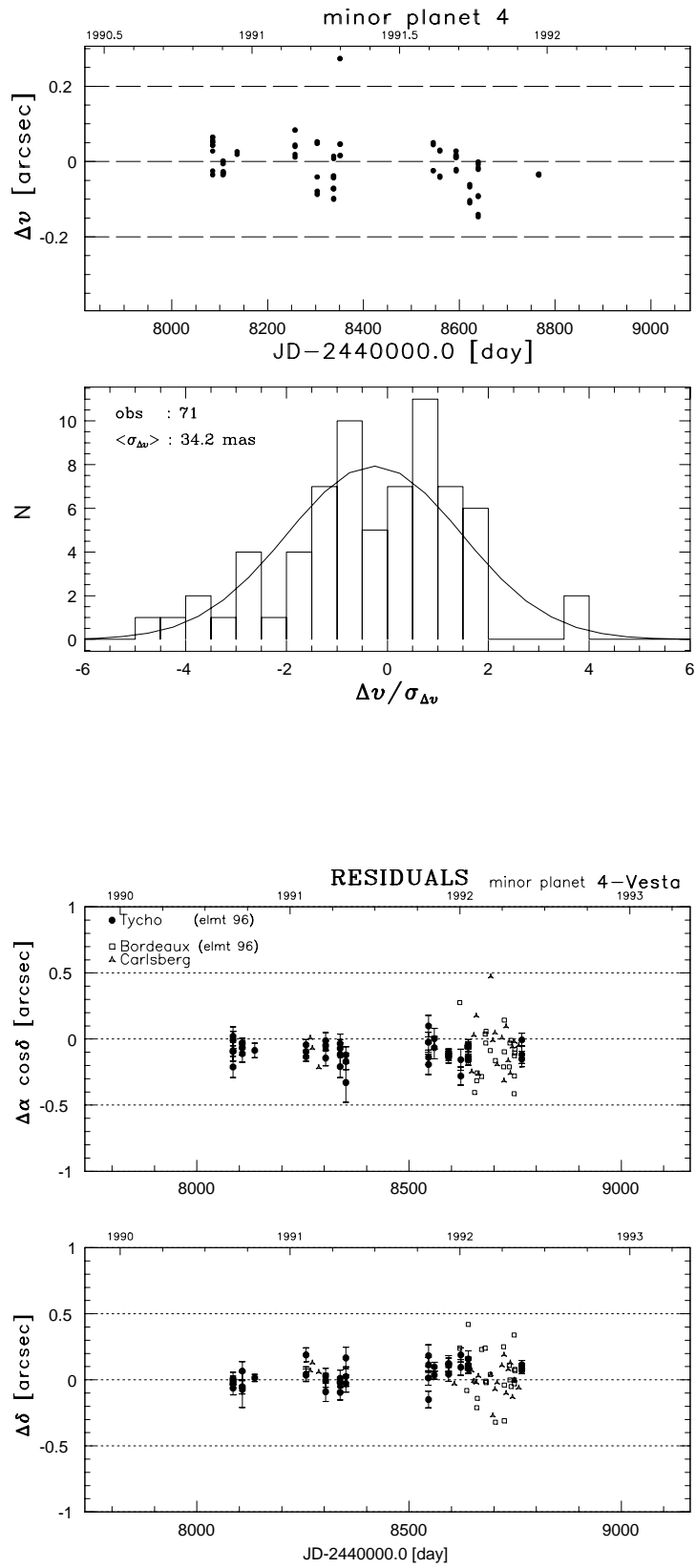


Figure 15.5. Same as Figure 15.3 for (4) Vesta.

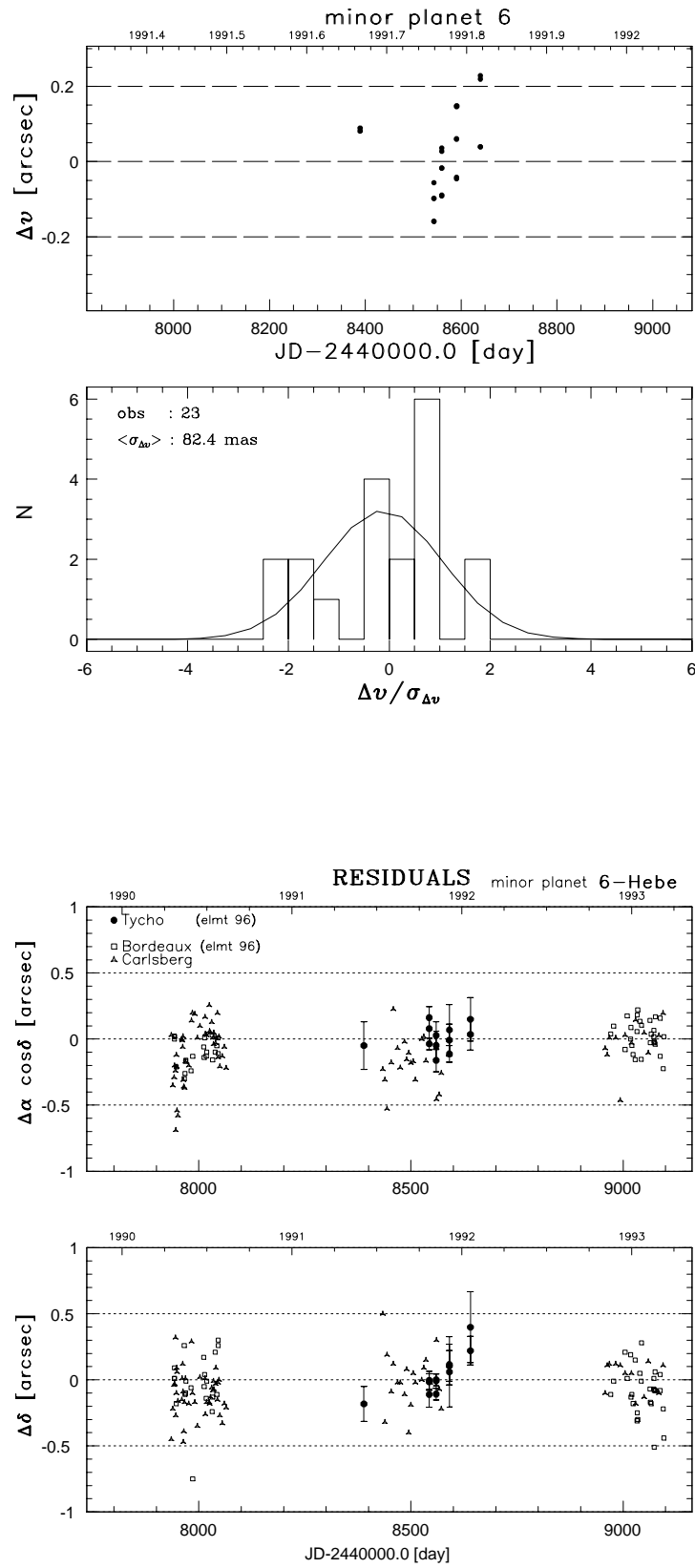
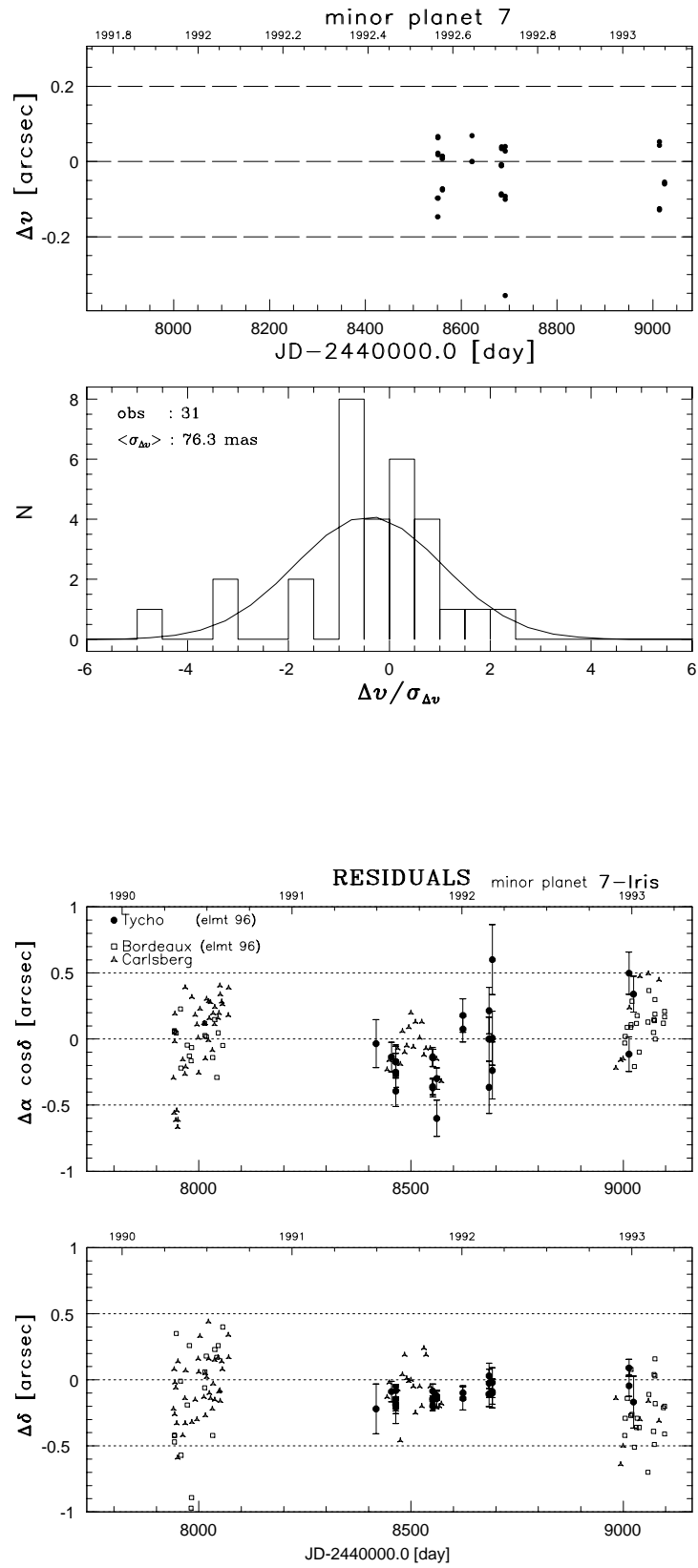
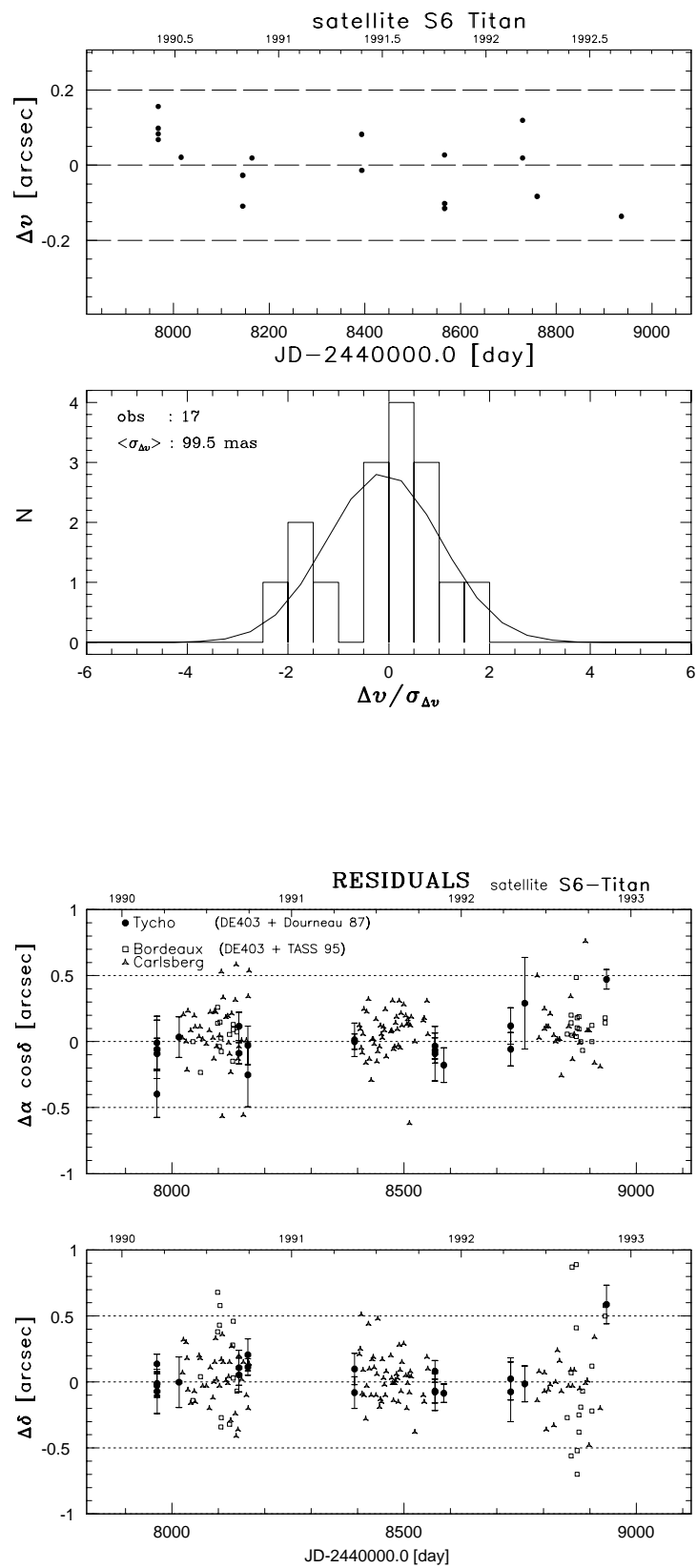


Figure 15.6. Same as Figure 15.3 for (6) Hebe.



**Figure 15.7.** Same as Figure 15.3 for (7) Iris.



**Figure 15.8.** Same as Figure 15.3 for the Saturnian satellite S VI-Titan.

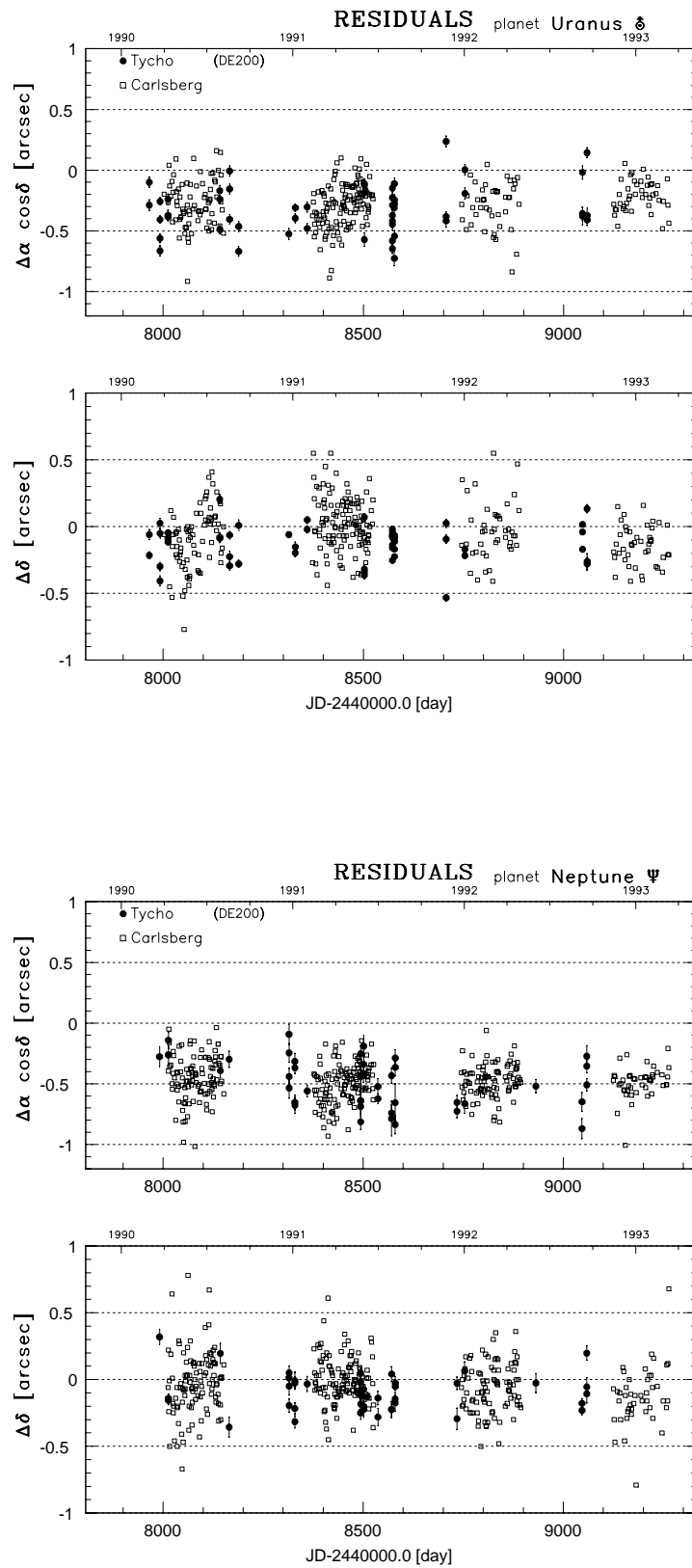


**Figure 15.9.** Residuals for Tycho observations of Uranus and Neptune, together with residuals obtained from Carlsberg instrument observations. The calculated positions are taken from the DE200 ephemeris solution.